Supporting Information

SEVI Inhibits Aβ Amyloid Aggregation by Capping the β-Sheet Elongation Edges

Ying Wang[1,2#], Jia Xu[3#], Fengjuan Huang[2], Jiajia Yan[1], Xinjie Fan[1], Yu Zou[4], Chuang Wang[3]*, Feng Ding[5*], Yunxiang Sun[1,2,5]*

1. School of Physical Science and Technology, Ningbo University, Ningbo 315211, China
2. Ningbo Institute of Innovation for Combined Medicine and Engineering (NIIME), Ningbo Medical Center Lihuili Hospital, Ningbo 315211, China
3. School of Medicine, Ningbo University, Ningbo 315211, China
4. Department of Sport and Exercise Science, Zhejiang University, Hangzhou 310058, China
5. Department of Physics and Astronomy, Clemson University, Clemson, SC 29634, United States

# Ying Wang and Jia Xu contributed equally to this work.

*E-mail: wangchuang@nbu.edu.cn, fding@clemson.edu, sunyunxiang@nbu.edu.cn

Table S1. The details of molecular systems in our DMD simulations, including the number of SEVI and Aβ peptides in each molecular system (No.); the corresponding dimensions of the cubic simulation box (Box size); the number of independent DMD simulation trajectories performed (DMD run); the length of each DMD simulation (Time) , and the accumulative total simulation time (Total time).

System	No.	Box size (nm)	DMD run	Time (μs)	Total time (μs)
SEVI	1	6.5	50	0.60	30.0
	2	7.5	50	1.20	60.0
Aβ	1	6.5	50	0.60	30.0
	2	7.5	50	1.20	60.0
SEVI & Aβ mixture	1&1	7.5	50	1.20	60.0
	2&2	9.5	50	1.20	60.0
Aβ(fibril) & SEVI	20&1	12.0	50	0.60	30.0

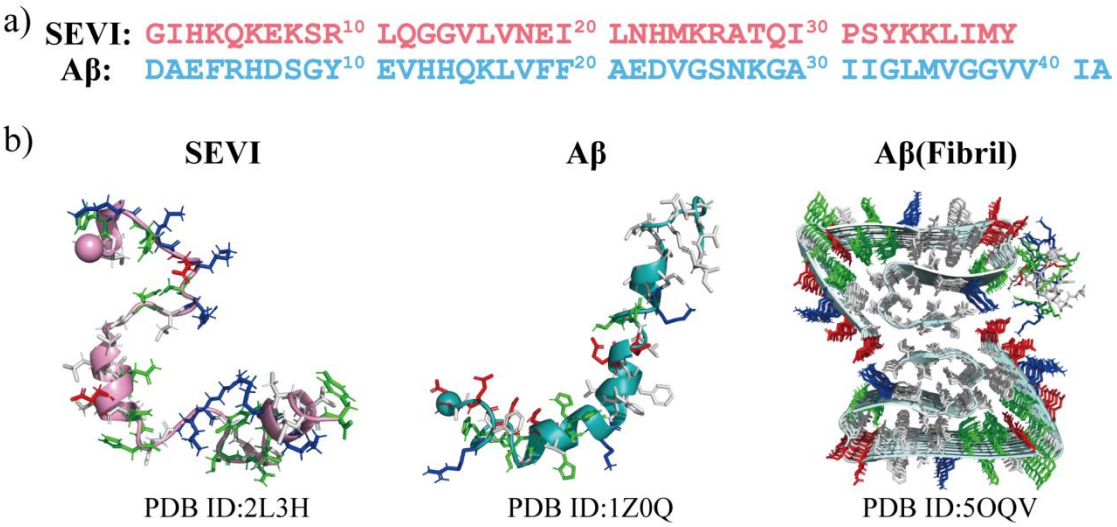

Figure S1. Amino acid sequences and structure of SEVI and Aβ. The primary amino acid sequences of SEVI and Aβ **a)**. The initial structures of the SEVI monomer, along with the Aβ monomer and proto-fibril used in our simulation **b)**. The proto-fibril of Aβ is composed of 20 peptides. Side-chains are shown sticks and colored by residue type: hydrophobic residues (white), negatively charged residues (red), positively charged residues (blue), and polar residues (green).

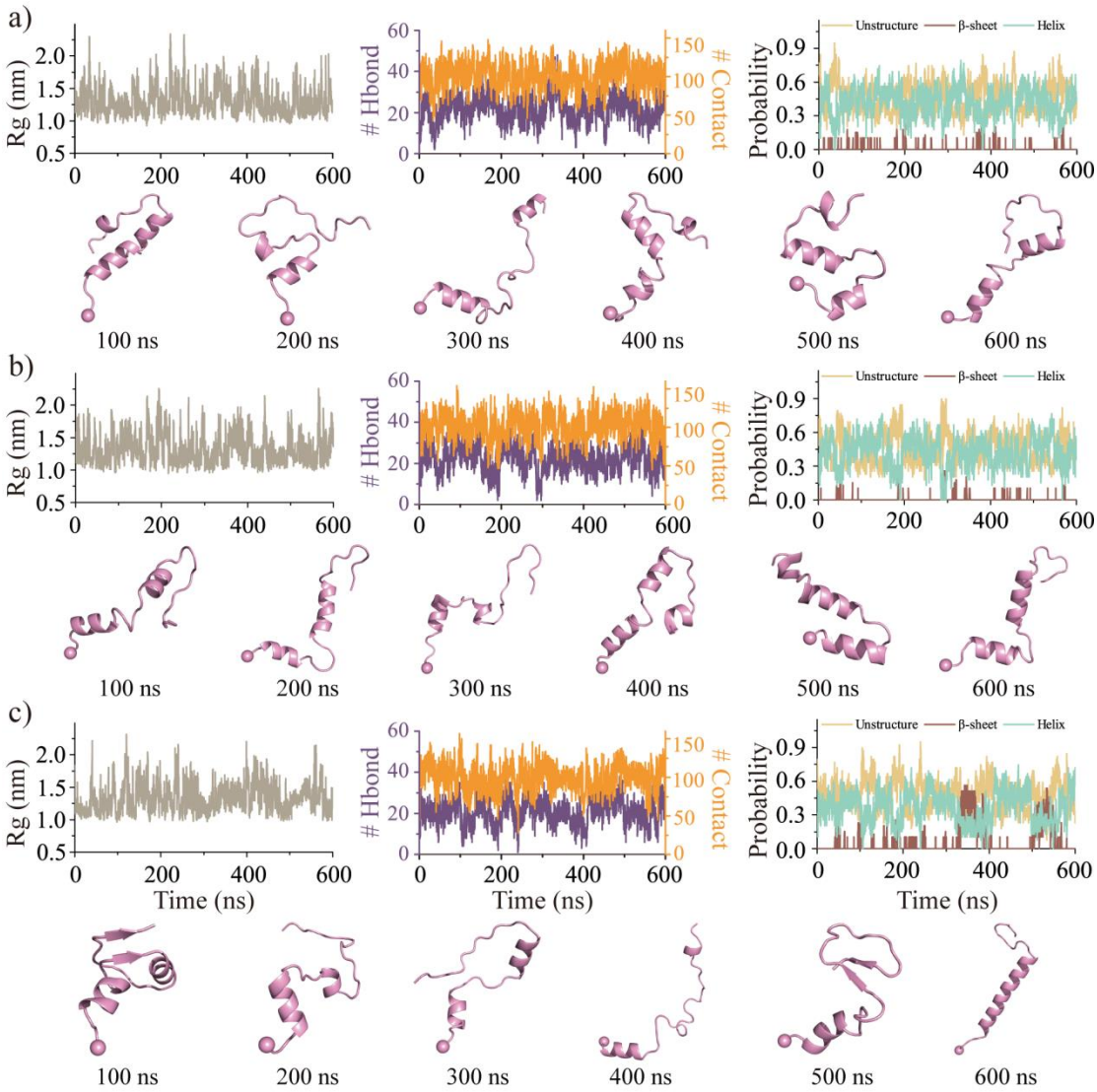

Figure S2. The conformational sampling efficiency and equilibrium assessments for the simulation of SEVI monomer. Time evolution of the radius gyration (Rg), the number of intra-molecular backbone hydrogen bonds and contacts, along with the probability of the structured (β-sheet and helix) and unstructured (random coil and bend) formations of SEVI monomer **a-c)**. The snapshots are presented every 100 ns according to the simulation time. The N-terminal Cα atom is highlighted as a bead. Three representative trajectories are randomly selected from fifty independent DMD simulations.

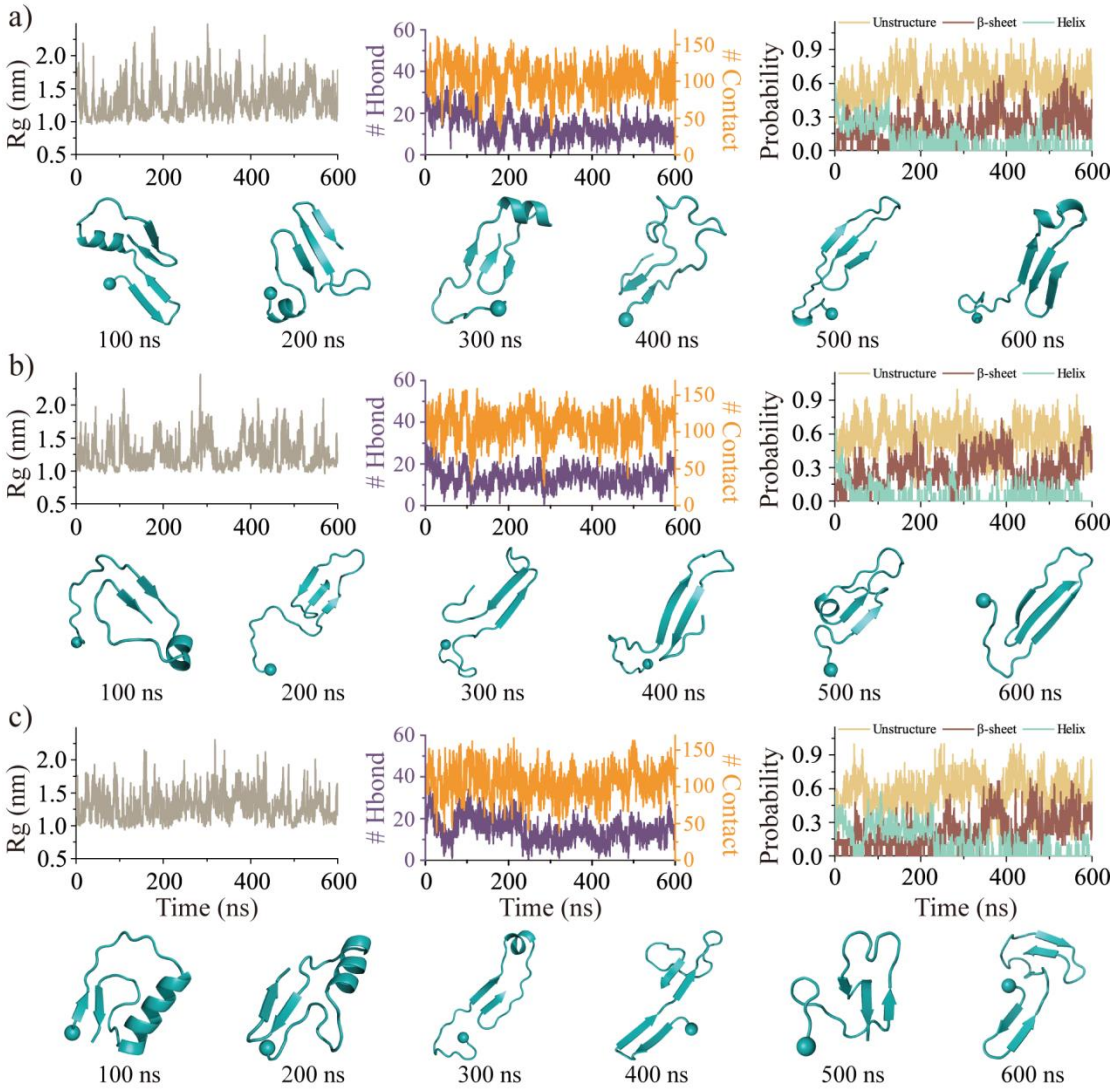

Figure S3. The conformational sampling efficiency and equilibrium assessments for the simulation of Aβ monomer. Time evolution of the radius gyration (Rg), the number of intra-molecular hydrogen bonds and contacts, along with the probability of the structured (β-sheet and helix) and unstructured (random coil and bend) formations of Aβ monomer **a-c)**. The snapshots are presented every 100 ns according to the simulation time. The N-terminal Cα atom is highlighted as a bead. Three representative trajectories are randomly selected from fifty independent DMD simulations.

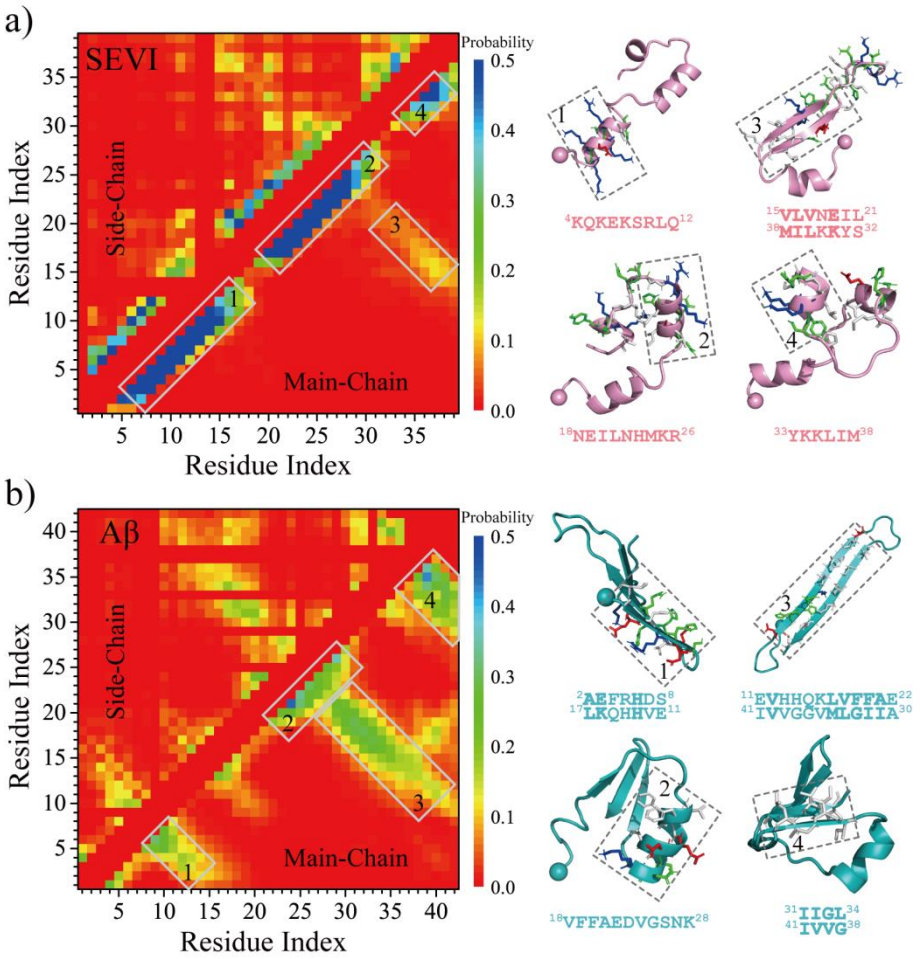

Figure S4. Residue-pairwise contact frequency of SEVI and Aβ monomer. The residue-pairwise intra-peptide contact frequency maps are computed between main-chain atoms (lower diagonal) and side-chain atoms (upper diagonal) of SEVI **a)** and Aβ **b)** monomer based on the last 300 ns data from fifty independent DMD trajectories. The representative structured motifs with high contact frequency patterns, mostly corresponding to the helices or β-sheets labeled as 1–4 in the contact frequency map, are also presented on the right. Side-chain within the helical and β-hairpin motifs are shown as sticks and colored according to the residue type (hydrophobic residues (white), negatively charged residues (red), positively charged residues (blue), and polar residues (green)).

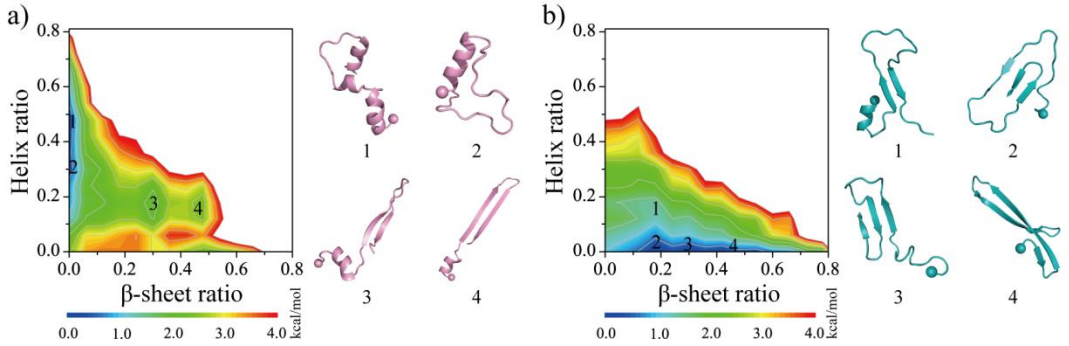

Figure. S5. The conformational free energy landscape of SEVI and Aβ monomers. The potential mean force as a function of β-sheet and helix contents of the monomeric SEVI **a)** and Aβ **b)**. Four representative structures labeled in the PMFs are also shown on the right. The SEVI and Aβ are colored pink and cyan, respectively.

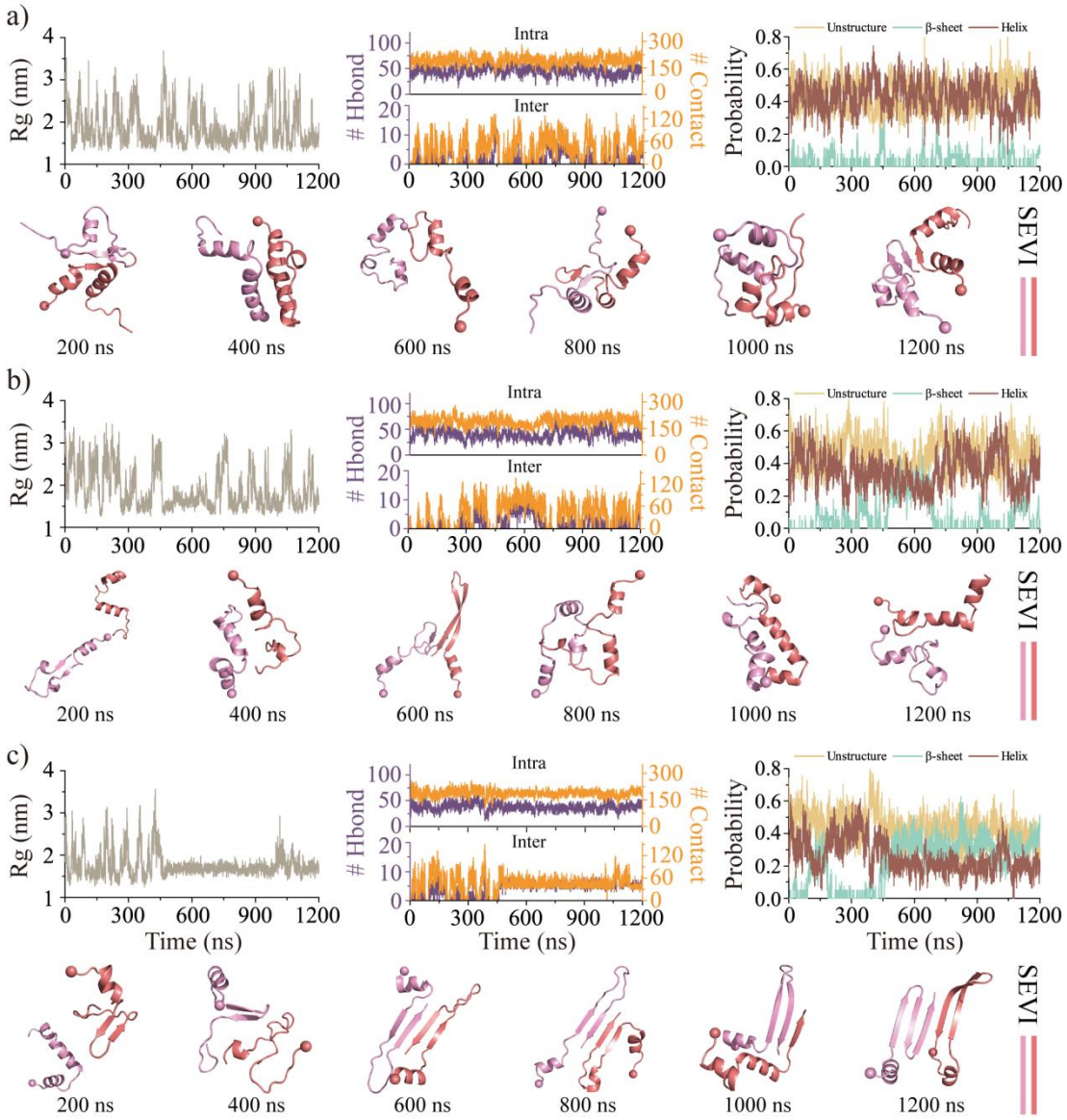

Figure S6. The conformational sampling efficiency assessments and equilibrium analyses for the homo-dimerization simulation of SEVI peptides. Time evolution of the radius gyration (Rg), the number of hydrogen bonds and contacts, along with the probability of the unstructured (random coil and bend) and structured (helix and β-sheet) formations in the two-peptide simulations of SEVI **a-c)**. Three representative trajectories are randomly selected from fifty independent DMD simulations. The N-terminal Cα atom of each peptide is highlighted as a bead.

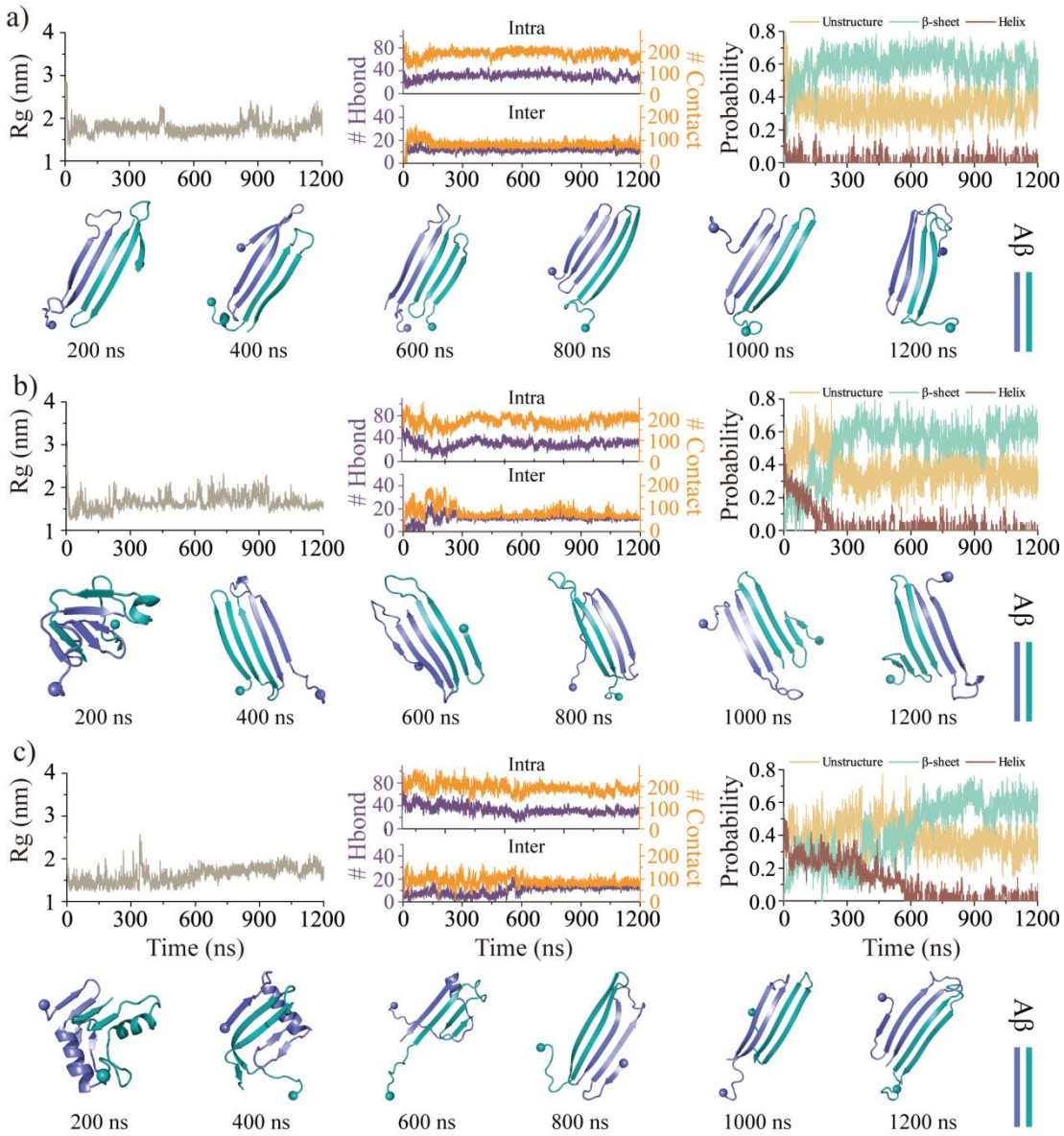

Figure S7. The conformational sampling efficiency assessments and equilibrium analyses for the homo-dimerization simulation of Aβ peptides. Time evolution of the radius gyration, the number of hydrogen bonds and contact, along with the probability of the unstructured (random coil and bend) and structured (helix and β-sheet) formations in the two-peptide simulations of Aβ **a-c)**. Three representative trajectories are randomly selected from fifty independent DMD simulations. The N-terminal Cα atom of each peptide is highlighted as a bead.

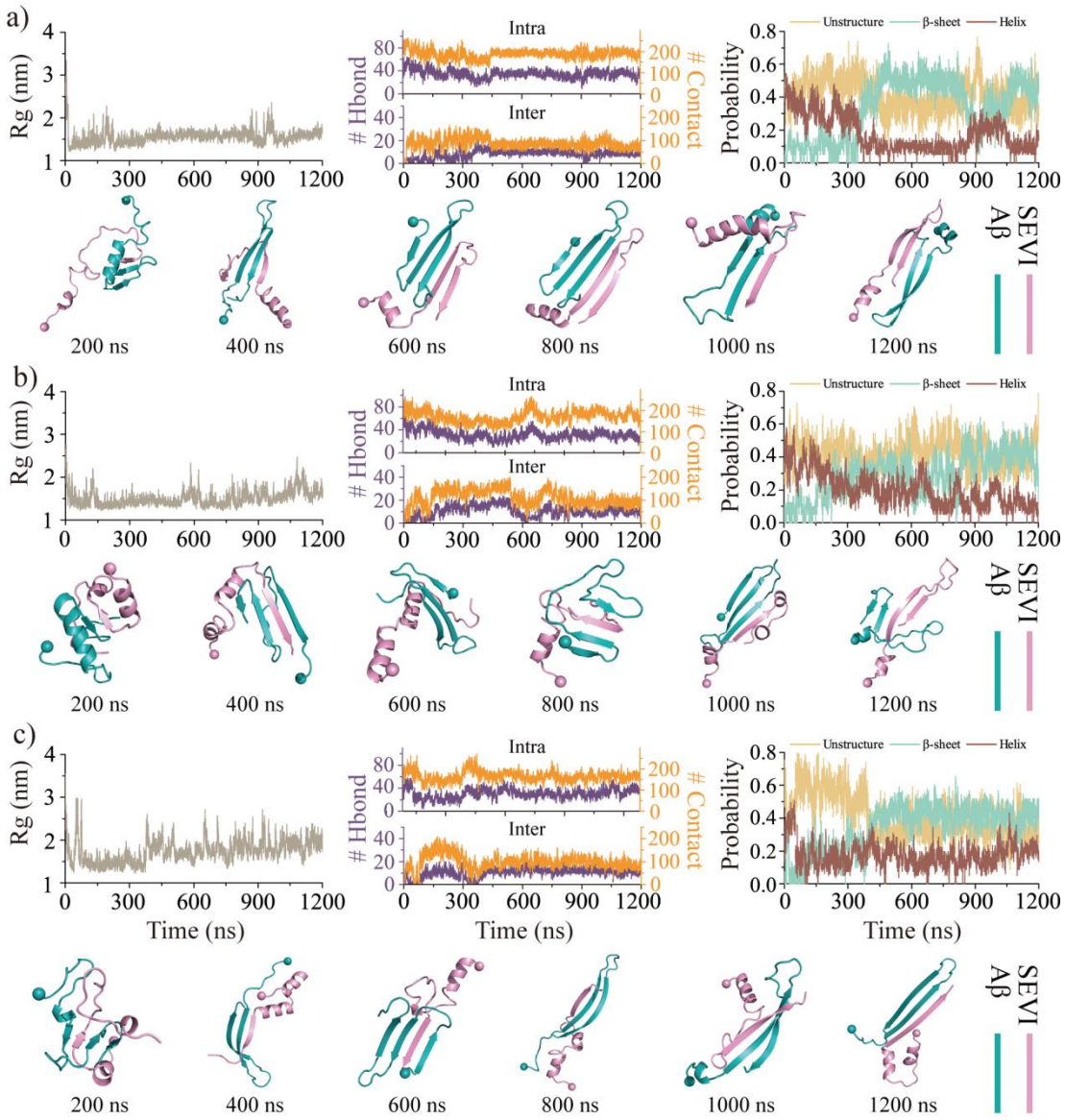

Figure S8. The conformational sampling efficiency assessments and equilibrium analyses for the hetero-dimerization simulation of one SEVI mixed with one Aβ. Time evolution of the radius gyration, the number of hydrogen bonds and contact, along with the probability of the unstructured (random coil and bend) and structured (helix and β-sheet) formations in the SEVI and Aβ mixed hetero-dimerization simulations **a-c)**. Three representative trajectories are randomly selected from fifty independent DMD simulations. The N-terminal Cα atom of each peptide is highlighted as a bead. The SEVI and Aβ peptides are colored pink and cyan, respectively.

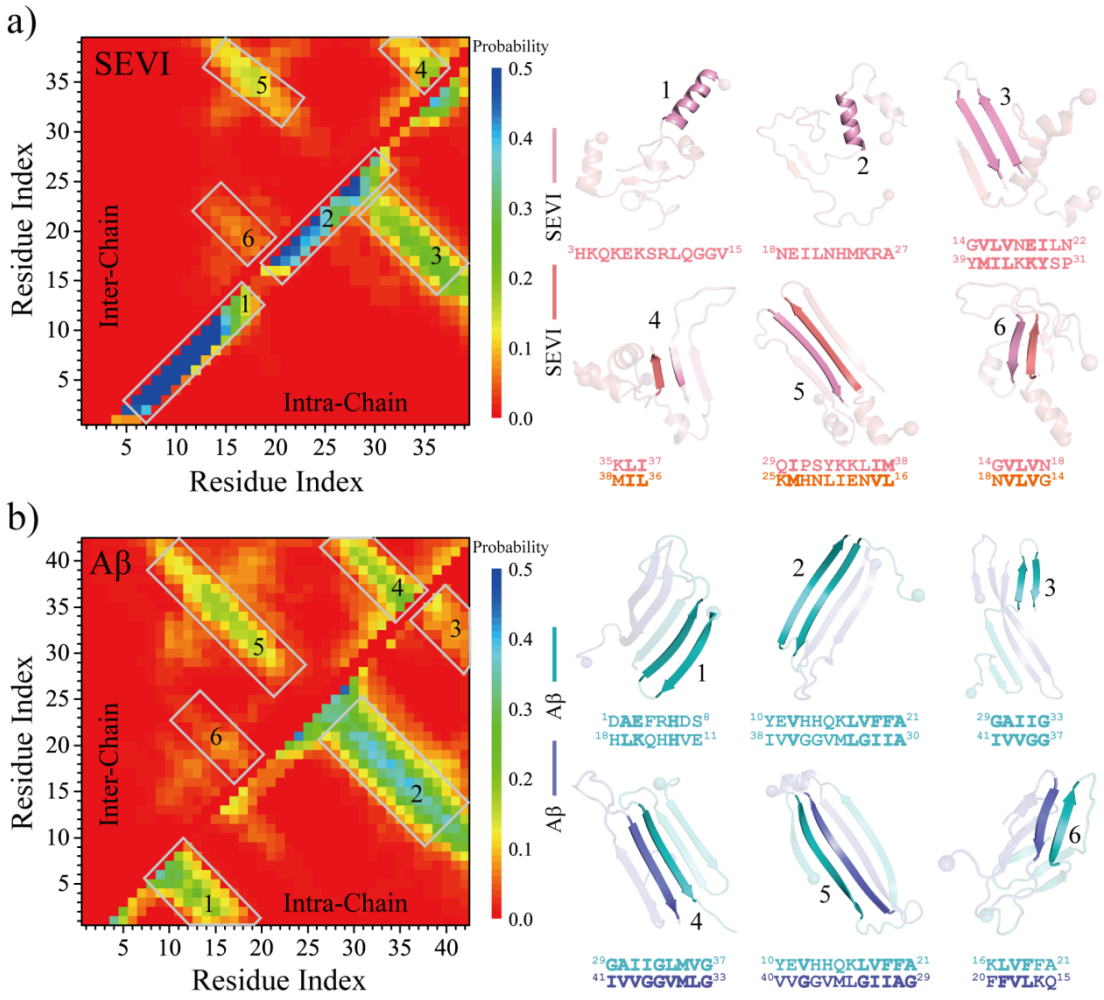

Figure S9. Residue-pairwise contact frequency of SEVI and Aβ homo-dimer. The intra-chain and inter-chain residue-pairwise contact frequencies of SEVI **a)** and Aβ **b)** homo-dimer are calculated using the last 600 ns saturated conformations from fifty independent DMD simulations. The representative structured motifs with high contact frequency patterns labeled as 1–6 in the contact frequency map are also presented on the right. For clarity, the two SEVI are colored red and pink, and two Aβ are colored by blue and cyan.

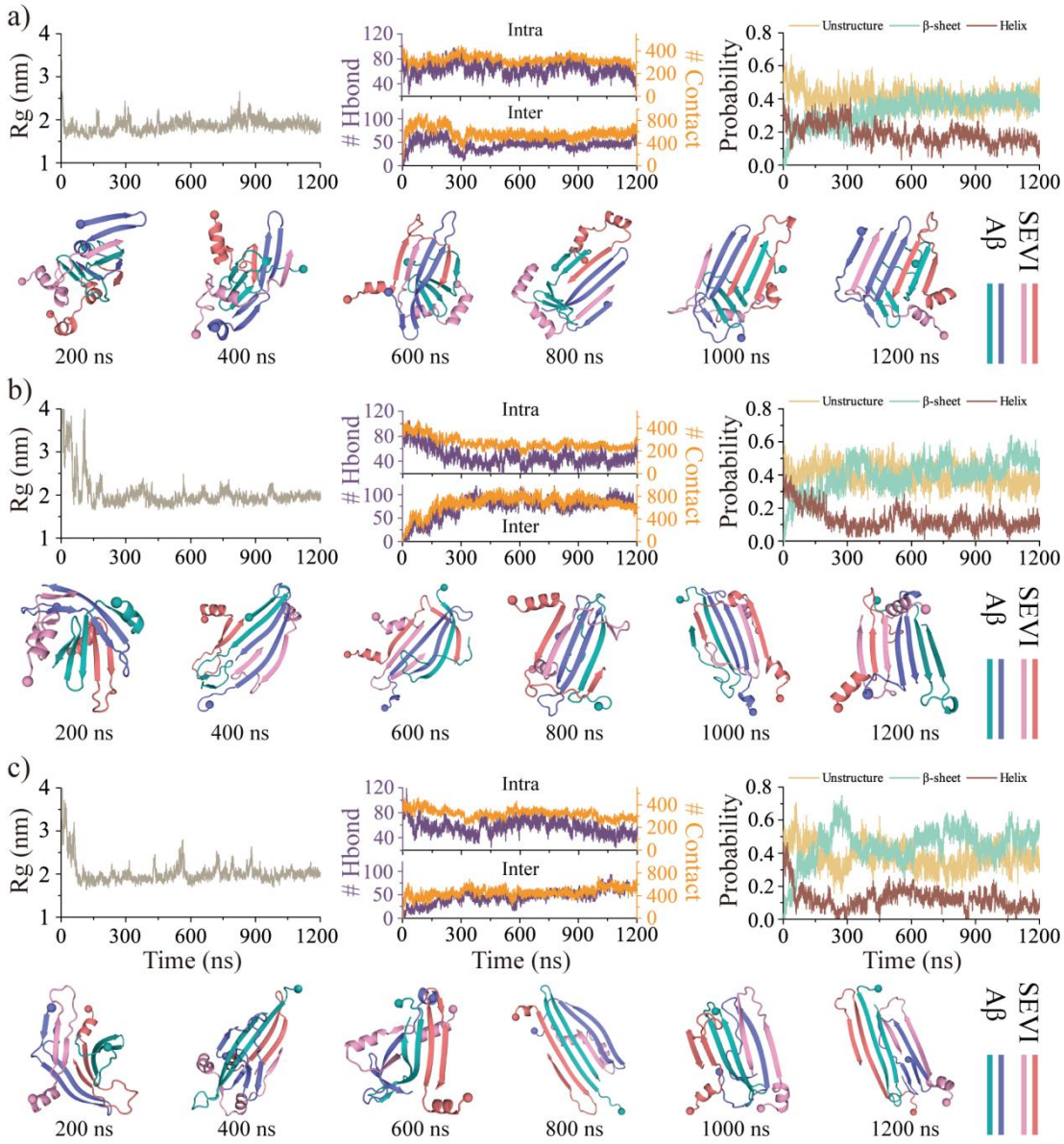

Figure S10. The conformational sampling efficiency assessments and equilibrium analyses for the simulation of two SEVI mixed with two Aβ peptides. Time evolution of the radius gyration (Rg), the number of hydrogen bonds and contacts, along with the probability of the unstructured (random coil and bend) and structured (helix and β-sheet) formations in the simulations of two SEVI mixed with two Aβ peptides **a-c)**. Three representative trajectories are randomly selected from fifty independent DMD simulations. The N-terminal Cα atom is highlighted as a bead. The SEVI are peptides colored pink and red, and the Aβ peptides are colored blue and cyan, respectively.

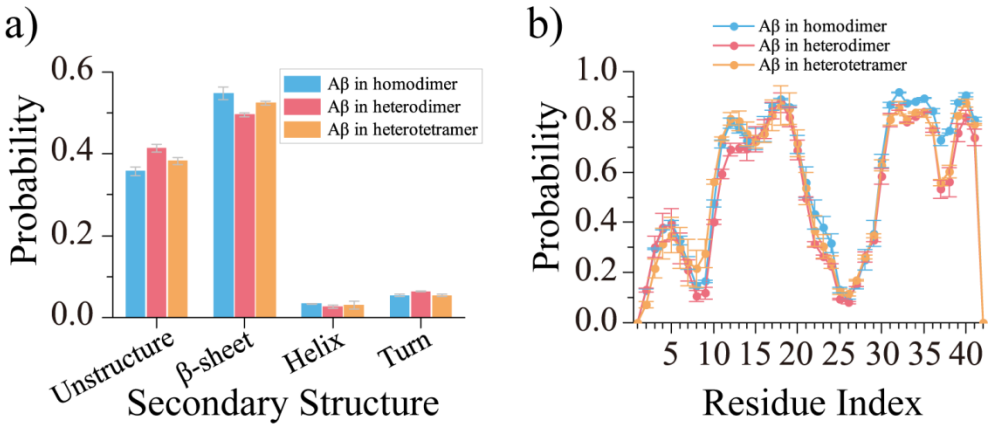

Figure S11. Effects of SEVI on the β-sheet structure of Aβ42 in their hetero-aggregates. Average secondary structure content of Aβ42 in homo-dimer, hetero-dimer, and hetero-tetramer **a)**. Average β-sheet propensity of each residue of Aβ42 in homo-dimer, hetero-dimer, and hetero-tetramer **b)**.

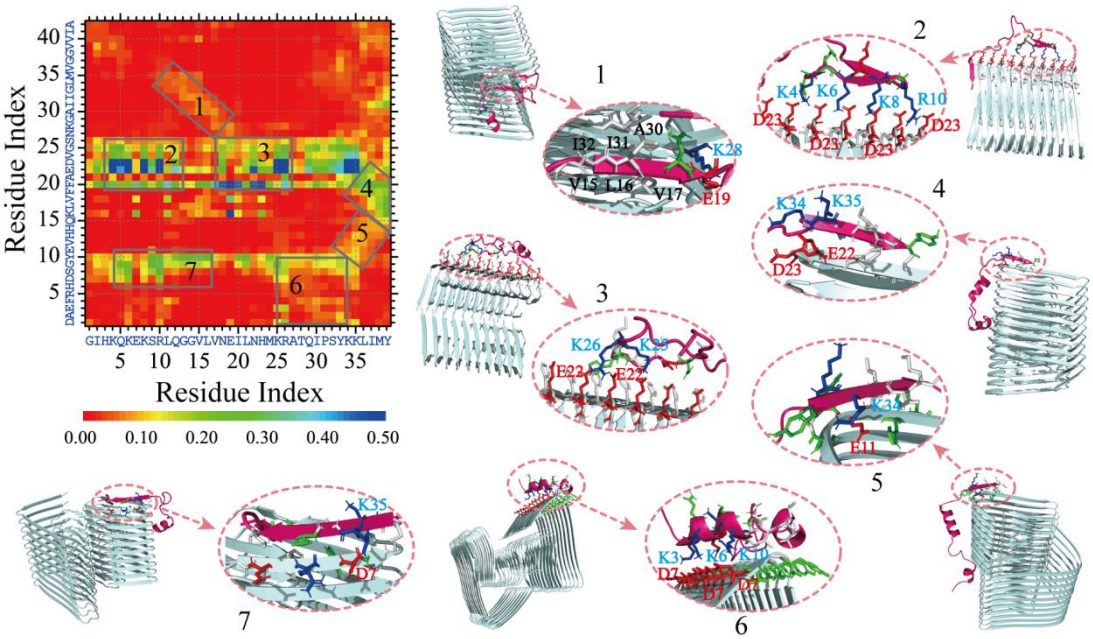

Figure S12. The interaction of SEVI monomer and Aβ proto-fibril analysis. The residue-pairwise contact frequency between SEVI monomer and Aβ proto-fibril. Representative binding modes and corresponding structures are labeled as 1-7 in the residue-pairwise contact map and presented.